

# On characterising fracture resistance in mode-I delamination

Leo ŠKEC\*, Giulio ALFANO<sup>+</sup>, Gordan JELENIĆ\*

\**University of Rijeka, Faculty of Civil Engineering, Radmile Matejčić 3, 51000 Rijeka, Croatia*

*E-mails: [leo.skec](mailto:leo.skec@uniri.hr), [gordan.jelenic](mailto:gordan.jelenic@uniri.hr)@uniri.hr*

<sup>+</sup>*Brunel University London, Kingston Lane, UB8 3PH, Uxbridge, UK*

*E-mail: [giulio.alfano@brunel.ac.uk](mailto:giulio.alfano@brunel.ac.uk)*

***Abstract.** In this work we focus on the mode-I quasi-static crack propagation in adhesive joints or composite laminates. For this problems a number of different standards have been approved. The most widely used are based on the double cantilever beam (DCB) test and on linear elastic fracture mechanics (LEFM) but differ in some aspects of the testing procedure and the recommended data-reduction schemes. The applicability of these methods is still a matter of debate in the scientific community, particularly in the case of ductile interfaces. We revisit the accuracy of the most used standards and compare it with other methods based on either LEFM or J-integral theory. All the methods analysed in our work are based on either Euler-Bernoulli or Timoshenko beam theories. We present a number of numerical examples where we compare different expressions for fracture resistance obtained with different methods. The input for the analysis, which includes applied load, cross-head displacement and rotation, crack length and cohesive zone length, is obtained from the numerical model which simulates real experiments. In these simulations, we use a Timoshenko beam model with a bi-linear CZM, which allows us accurate comparison with analytical formulas for fracture resistance based on Euler-Bernoulli and Timoshenko beam theory.*

## 1 Introduction

In recent years, the use of linear elastic fracture mechanics (LEFM) for the experimental determination of the fracture resistance during adhesive joint debonding or composite delamination in presence of 'large-scale' fracture processes, has been seriously questioned. In general, it is widely accepted that "LEFM is not applicable to those specimens containing large fracture process zone around the delamination front" [1]. Instead, there is a general consensus that, in presence of large process zones, J-integral theory [2] provides a more accurate framework to determine the fracture resistance [3].

Because for the aforementioned types of problems, a very accurate characterisation of the fracture cannot be obtained using a one-parameter fracture-mechanics theory, the richer modelling framework of cohesive-zone models (CZMs) is an alternative that is usually considered [4]. In this work we will consider the critical energy release rate,  $G_c$ , the critical value of the J integral,  $J_c$ , and the area under the traction separation law  $\Omega$  as candidates to characterise fracture resistance by a single energy value. Because, in the general case,  $\Omega$  is the only parameter that can be considered as an interface property, we

will assess the accuracy of methods based on either  $G_c$  or  $J_c$  by evaluating how closely they predict  $\Omega$ .

When it comes to mode-I delamination or debonding, today we have many different standard procedures for determining the fracture resistance of adhesive joints and composite laminates [5], [6]. Due to its simple geometry and a rather simple testing procedure used, the double cantilever beam (DCB) is the most commonly used specimen in all the standards. All standards use analytical formulae to compute  $G_c$  based on LEFM and simple beam theories (Euler-Bernoulli or Timoshenko), where it is assumed that the DCB arms are clamped at the crack tip. Furthermore, in order to compute  $G_c$ , the measurement of the crack length, which is usually done optically by means of a travelling microscope or a high-resolution camera, is required. However, determining the exact position of the crack tip is extremely difficult and time-consuming, and it can introduce significant uncertainty in the determination of  $G_c$ . Although formulae for  $G_c$  that do not require measurement of the crack length have been already proposed in the literature [7], [8], they do not take into account the difference between the actual crack length,  $a$ , and the equivalent crack length,  $a_{eq}$ , which is the length that makes simple beam deflection formulae valid for a measured pair of force and displacement.

In this work we first discuss the difference between  $G_c$ ,  $J_c$  and  $\Omega$  in Section 2. Then, for the case of a DCB with prescribed displacement, in Section 3 we derive the correct formula for  $G_c$ . Using the numerical data produced from ‘virtual’ experiments, the accuracy of different formulae for  $G_c$  and  $J_c$  is compared in Section 4. Finally, the most important conclusions are presented in Section 5. This work is a brief summary of [9], where a more detailed discussion about the J integral, the case of DCB with prescribed rotations and additional numerical comparisons can be found.

## 2 Relationship between $G_c$ , $J_c$ and $\Omega$

Let us consider the case of a DCB specimen that is modelled as a 2D solid pinned in two points, subject to a monotonically increasing prescribed (opening) displacement,  $v$ , on one of its pinned ends as shown in Figure 1. An initial crack of length  $a_0$  is assumed to be present in a plane of geometric, material and loading symmetry of the body so that crack propagates in pure mode I.

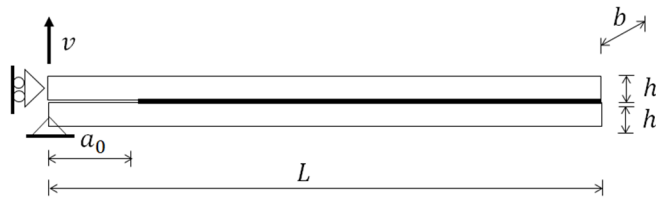


Figure 1: Geometry of a DCB with prescribed displacement

The interface of the DCB considered is modelled with the CZM shown in Figure 2(a) where the behaviour is linear elastic with progressive damage. As clarified in Figure 2(a),  $\delta_0$  and  $\delta_c$  are the limit values of the relative displacement,  $\delta$ , at the interface, whereas  $\sigma_{max}$  is the limit value of the contact traction  $\sigma$ . It is very important to notice

that in a DCB new damage dissipation occurs only ahead of the crack tip on the part of the interface where  $\delta_0 < \delta \leq \delta_c$ . Once  $\delta_c$  is reached all the energy,  $\Omega$ , is dissipated (see Figure 2(b)).

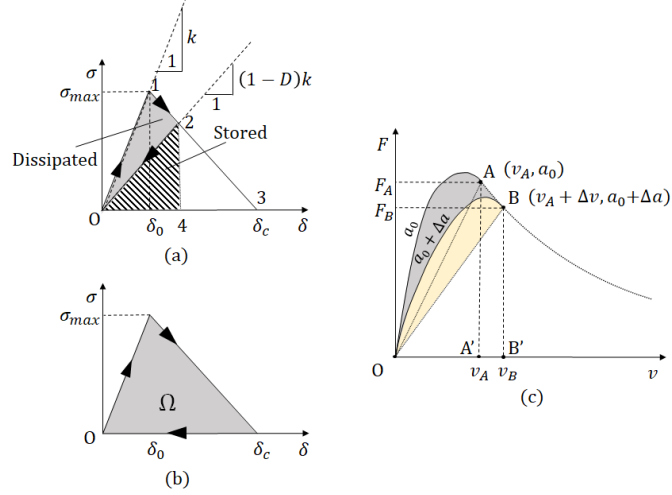


Figure 2: DCB with a bi-linear CZM with progressive failure: traction separation law for (a) a partially damaged point and (b) a fully damaged point, and (c) the associated structural response

When the body with an initial crack  $a_0$  reaches the force  $F_A$  and the displacement  $v_A$ , which is the point at which  $\delta$  reaches  $\delta_c$  at the initial crack tip, the triangle OAA'O represents the part of the external work stored as elastic energy, which in this case is the total potential energy  $\Pi_A$ , whereas the part OAO (where OA is a curve and AO a straight line) is energy dissipated due to damage at the interface ahead of the crack tip, and will be here denoted by  $\Pi_{D,A}$ . As soon as at the crack tip  $\delta = \delta_c$ , the crack will start propagating if the prescribed displacement is further increased. In other words, when the prescribed displacement is  $v_B > v_A$ , the crack length will become  $a_0 + \Delta a$ , while the force decreases from  $F_A$  to  $F_B$ . The potential energy stored at point B,  $\Pi_B$ , is the area of the triangle OBB'O.

The unloaded body from point B would not be the same as one with an initial crack equal to  $a_0 + \Delta a$ , because the latter would have no damage developed ahead of the crack tip. The area OBO (where OB is a curve and BO is a straight line), shaded in yellow in Figure 2(c), represents the energy dissipated ahead of the crack tip at point B when the linear elastic CZM with progressive failure is used, and is therefore denoted by  $\Pi_{D,B}$ . Grey area in Figure 2(c) represents the energy dissipated on a newly created crack surface. In general, at all times during crack propagation the total (nonlinear) potential energy,  $\Pi_{NL}$ , can be written as

$$\Pi_{NL} = \Pi + \Pi_D \quad (1)$$

where, as discussed above,  $\Pi$  is the energy stored, while  $\Pi_{NL}$  is the energy dissipated ahead of the crack tip. As shown in [9], we can derive the following relation:

$$\Omega = -\frac{1}{b} \frac{\partial \Pi_D}{\partial a} - \frac{1}{b} \frac{d\Pi_D}{da} = G_c - \frac{1}{b} \frac{d\Pi_D}{da}, \quad (2)$$

or, for the case of an homogeneous material, where  $\Omega = J_c$ ,

$$J_c = G_c - \frac{1}{b} \frac{d\Pi_D}{da}. \quad (3)$$

The above results show that the difference between  $G_c$  and  $\Omega$ , and between  $G_c$  and  $J_c$  for a homogeneous interface, is not to be attributed to the size of the cohesive zone, but to the variation of the amount of energy already dissipated ahead of the crack tip during crack propagation. In other words, if the profile of the specific energy dissipated ahead of the crack tip remains unaltered during crack propagation, and therefore translates in a steady-state fashion together with the crack tip, then  $G_c = J_c = \Omega$ . It is worth mentioning, that in [9] it has been shown that for a case of a non-homogeneous interface (which can be modelled as variable  $\Omega$  over the interface),  $J_c \neq \Omega$ .

### 3 Determination of $G_c$ for a DCB with prescribed displacement

We will assume that the DCB (as shown in Figure 1) is a 2D body undergoing an isothermal, quasi-static, rate-independent deformation process, where the length, width and depth of each arm are denoted by  $L$ ,  $b$  and  $h$ , respectively, with  $h \ll L$ . We will also assume that strains, displacements and rotations are sufficiently small so that a geometrically linear beam model is sufficiently effective. Because the behaviour is linear elastic with damage, using geometrically linear beam theories, the total potential energy is given by

$$\Pi(v, a) = \frac{Fv}{2}, \quad (4)$$

where  $F = F(v, a)$  is the reaction force.

$F$ ,  $v$  and  $a$  can be related using formulae from simple beam theories, but we have to be aware that the crack length in these formulae is not the actual crack length  $a$ , but an equivalent crack length, which will be denoted by  $a_{eq.E}$  or  $a_{eq.T}$  to specify that Euler-Bernoulli or Timoshenko beam theory is considered, respectively. Beam deflection formulae are based on the assumption that the arms of the DCB are clamped at the crack tip, but cross sections at the crack tip are normally characterised by both a displacement and a rotation as a result of the deformation of the interface and of the beam in front of the crack tip. Therefore, the equivalent crack length is defined as the length that the crack should have to make the formulae correct if the arms were really clamped at the crack tip, for given values of  $F$  and  $v$ .

For Euler-Bernoulli beam theory we have

$$a_{eq.E} = \sqrt[3]{\frac{3vEI}{2F}}, \quad (5)$$

where  $EI$  is the bending stiffness of a single DCB arm. Because the total potential energy can be now expressed as

$$\Pi(v, a) = \Pi_E(v, a_{eq.E}(a)), \quad (8)$$

we can derive

$$G_c = -\frac{1}{b} \frac{\partial \Pi}{\partial a} = -\frac{1}{b} \frac{\partial \Pi_E}{\partial a_{eq,E}} \frac{\partial a_{eq,E}}{\partial a}, \quad (9)$$

which can be written as

$$G_c = G_c^E \frac{\partial a_{eq,E}}{\partial a}, \quad (10)$$

where

$$G_c^E = \frac{F^2 a_{eq,E}^2}{b EI}. \quad (11)$$

The derivative  $\frac{da_{eq,E}}{da}$  in Equation (10) also defines how close to being steady state the crack propagation is. Therefore, for  $\frac{da_{eq,E}}{da} = 1$ , we have  $G_c = J_c = \Omega$ , which, as shown in [9], is the case for a DCB with prescribed rotations. Analogous procedure can be applied also for Timoshenko beam theory, as shown in [9].

#### 4 Numerical Examples

By using a DCB numerical model [10] consisting of Timoshenko beam finite elements with an interface with a bi-linear CZM (see Figure 2(a)), we created ‘virtual’ experimental data ( $F$ ,  $v$  and  $a$ ), which are then used in various formulae for  $G_c$  and  $J_c$ . In our numerical model  $\Omega$  is a known input value. By keeping  $\Omega$  constant and changing  $\sigma_{max}$  (and  $\delta_c$ ), we can obtain a range of behaviours at the interface, which vary from an extremely brittle one to a extremely ductile one (with a relatively large damage process zone). All the data used in the numerical examples are given in Tables 1 and 2, where  $E$  represents the Young’s modulus,  $\nu$  is Poisson’s ratio (shear stiffness is computed as  $\mu = \frac{E}{2(1+\nu)}$ ) and  $k_s$  is the shear correction coefficient.

Table 1: Geometric data used in the virtual experiments

$L$	$h$	$b$	$a_0$
[mm]	[mm]	[mm]	[mm]
200	6	25	25

Table 2: Material data used in the virtual experiments

$E$	$\nu$	$k_s$	$\Omega$	$\sigma_{max}$	$\delta_c$	$\delta_0$
[GPa]	[-]	[-]	[N/mm]	[MPa]	[mm]	[mm]
70	1/3	5/6	1	{7.5, 15, 30, 60, 120}	$2\Omega/\sigma_{max}$	$0.01 \delta_c$

In Figure 3, values of  $G_c^E$  (as defined in Equation (11)) and  $da_{eq,E}/da$  are given for different values of  $\sigma_{max}$ . It can be noted that as  $\sigma_{max}$  increases the behaviour at the interface becomes more brittle and the crack propagation becomes extremely close to being steady state. In the limit case ( $\sigma_{max} \rightarrow \infty$ ),  $\frac{da_{eq,E}}{da} = 1$  and  $G_c^E = G_c = \Omega$ . However, even for the most ductile case ( $\sigma_{max} = 7.5$  MPa), we can see that the crack

propagation is very close to being steady state and  $G_c^E$  is indeed a very good approximation of  $\Omega$ . Moreover, formula (11) for  $G_c^E$  does not require the measurement of the crack length.

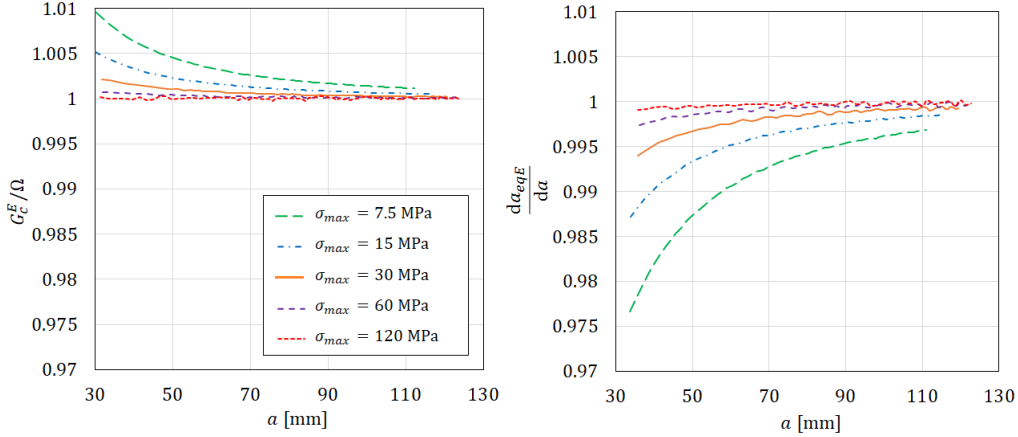


Figure 3: Values of (a)  $G_c^E / \Omega$  and (b)  $da_{eq,E} / da$  for different values of  $\sigma_{max}$

By multiplying  $G_c^E$  and  $da_{eq,E} / da$ , i.e. Figures 3(a) and 3(b), we get the actual value of  $G_c$ . In Figure 4(a) we can see that the same values of  $G_c$  are obtained regardless the beam theory used (EBT stands for Euler-Bernoulli, while TBT for Timoshenko beam theory). We can also see that as  $\sigma_{max} \rightarrow \infty$ ,  $G_c \rightarrow \Omega$ . In Figure 4(b), a comparison is made between different formulae for  $G_c$  and  $J_c$ , where, according to [9],

$$J_c^T = \frac{F^2}{b} \left( \frac{1}{\mu A_s} - \frac{2 \theta_v}{F} \right), \quad (12)$$

is the critical value of the J integral with shear deformability of the arms taken into account.  $\theta_v$  represents the rotation of the DCB arm at the point where the displacement  $v$  is prescribed. For Euler-Bernoulli beam theory,  $J_c^E$  is obtained by letting  $\mu A_s \rightarrow \infty$  in Equation (12). It can be noted that, for  $\theta_v$  obtained from a virtual experiment, Equation (12) for  $J_c^T$  is the only formula capable of giving the input value of  $\Omega$ .  $G_c^\Delta$  and  $\Omega^\Delta$  are values of  $G_c$  and  $\Omega$  computed using the areas under the  $F - v$  diagram, as discussed in Section 2. We can appreciate that the accuracy of all formulae presented in Figure 4(b) is very high, considering that the behaviour of the interface is extremely ductile.

## 5 Conclusions

In this work, for a case of a mode-I delamination in a DCB we derived the relationship between the critical energy released rate,  $G_c$ , the critical value of the J integral,  $J_c$ , and the area under the traction-separation law of a CZM,  $\Omega$ . We showed that, their difference is not to be attributed to the size of the damage process zone, but to how close to being steady state crack propagation is. As shown in Section 4, even for relatively large damage process zones, the difference between  $G_c$  (which is derived from LEFM) and  $\Omega$  is extremely small. Moreover, simple analytical formulae derived from LEFM and geometrically linear beam theories, namely  $G_c^E$  and  $G_c^T$ , are very accurate

approximations of  $\Omega$  that, unlike the formulae used in standards, do not require the measurement of the crack length.

In [9], a detailed derivation of the relationship between  $G_c$ ,  $J_c$  and  $\Omega$ , derivation of the expressions for  $G_c^T$ ,  $J_c^T$  and  $J_c^E$  can be found. Furthermore, the case of a DCB with prescribed rotations is investigated. Various numerical examples are presented where the accuracy of different expressions for  $G_c$  and  $J_c$  is assessed and compared with data-reduction schemes from standards.

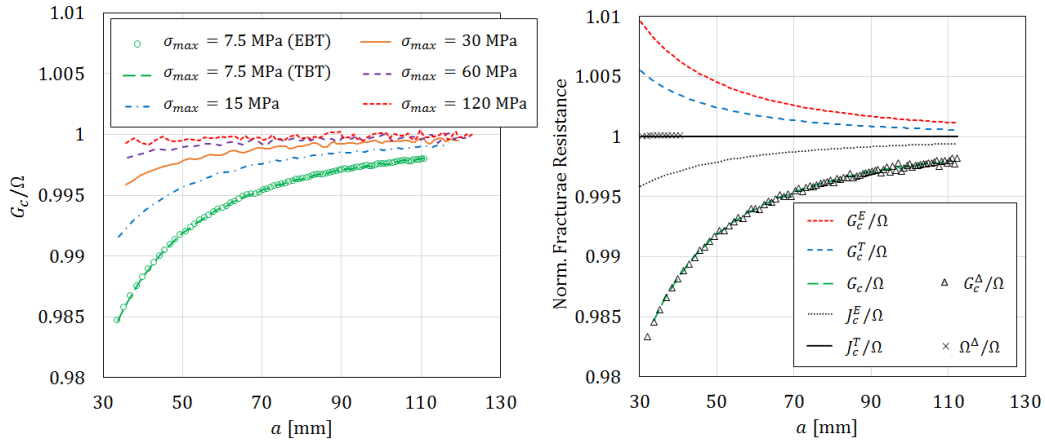


Figure 4: Values of: (a)  $G_c/\Omega$  for different values of  $\sigma_{max}$  and (b) different fracture resistance parameters normalised with respect to  $\Omega$  obtained for  $\sigma_{max} = 7.5$  MPa

### Supplementary data

Supplementary material related to this article can be found on-line at <http://dx.doi.org/10.17633/rd.brunel.6194483>.

### Acknowledgements

This project has received funding from the European Union’s Horizon 2020 research and innovation programme under the Marie Skłodowska-Curie grant agreement No. 701032. The third author wishes to acknowledge the financial support of the Croatian Science Foundation (Research Project IP-2016-06-4775).

### References

- [1] Z. Zhao, L. Seah, G. Chai. Measurement of interlaminar fracture properties of composites using the J-integral method. *Journal of Reinforced Plastics and Composites*, **35** (14): 1143–1154, 2016.
- [2] J.R. Rice. A path independent integral and the approximate analysis of strain concentration by notches and cracks. *Journal of Applied Mechanics*, **35**: 379–386, 1968.
- [3] T.L. Anderson. *Fracture Mechanics – Fundamentals and Applications*, 2<sup>nd</sup> Edition. CRC Press, Boca Raton, 1985.
- [4] B.F. Sørensen, T.K. Jacobsen. Determination of cohesive laws by the J integral approach. *Engineering Fracture Mechanics*, **70**: 1841–1858, 2003.

- [5] BS ISO 25217:2009. Adhesives –Determination of the Mode I Adhesive Fracture Energy of Structural Adhesive Joints Using Double Cantilever Beam and Tapered Double Cantilever Beam Specimens. *British Standard*, 2009.
- [6] ASTM D3433-99(2012). Standard Test Method for Fracture Strength in Cleavage of Adhesives in Bonded Metal Joints. *ASTM International*, 2012.
- [7] A. Biel, U. Stigh. An analysis of the evaluation of the fracture energy using the DCB-specimen. *Archives of Mechanics*, **59** (4-5): 311–327, 2007.
- [8] M.F.S.F. de Moura, R.D.S.G. Campilho, J.P.M. Gonçalves. Crack equivalent concept applied to the fracture characterization of bonded joints under pure mode I loading. *Composites Science and Technology*, **68**: 2224–2230, 2008.
- [9] L. Škec, G. Alfano, G. Jelenić. On  $G_c$ ,  $J_c$  and the characterisation of the mode-I fracture resistance in delamination or adhesive debonding. *International Journal of Solids and Structures*, **144-145**: 100-122, 2018.
- [10] L. Škec, G. Jelenić, N. Lustig. Mixed-mode delamination in 2D layered beam finite elements. *International Journal for Numerical Methods in Engineering*, **104**: 767–788, 2015.